Prostate Cancer Detection Using Crawling Wave Sonoelastography

Benjamin Castaneda[a,b]*, Liwei An[a], Shuang Wu[a], Laurie L. Baxter[c], Jorge L. Yao[c], Jean V. Joseph[d], Kenneth Hoyt[e], John Strang[f], Deborah J. Rubens[f], Kevin J. Parker[a]

[a]Department of Electrical & Computer Eng., University of Rochester, Rochester, NY, USA 14627; [b]Grupo de Formación y Procesamiento de Imágenes Médicas, Sección Electricidad y Electrónica, Departamento de Ingeniería, Pontificia Universidad Católica del Perú, Lima, Perú; [c]Department of Pathology & Lab Medicine, University of Rochester Medical Center, Rochester, NY, USA 14642; [d]Department of Urology, University of Rochester Medical Center, Rochester, NY, USA 14642; [e]Department of Radiology, University of Alabama at Birmingham, Birmingham, AL, USA 35924; [f]Department of Imaging Sciences, University of Rochester Medical Center, Rochester, NY, USA 14642

ABSTRACT

Crawling wave (CrW) sonoelastography is an elasticity imaging technique capable of estimating the localized shear wave speed in tissue and, therefore, can provide a quantitative estimation of the Young's modulus for a given vibration frequency. In this paper, this technique is used to detect cancer in excised human prostates and to provide quantitative estimations of the viscoelastic properties of cancerous and normal tissues. Image processing techniques are introduced to compensate for attenuation and reflection artifacts of the CrW images. Preliminary results were obtained with fifteen prostate glands after radical prostatectomy. The glands were vibrated at 100, 120 and 140Hz. At each frequency, three cross-sections of the gland (apex, mid-gland and base) were imaged using CrW Sonoelastography and compared to corresponding histological slices. Results showed good spatial correspondence with histology and an 80% accuracy in cancer detection. In addition, shear velocities for cancerous and normal tissues were estimated as 4.75±0.97 m/s and 3.26±0.87 m/s, respectively.

Keywords: Elasticity imaging, tissue characterization, crawling wave sonoelastography, image processing, prostate cancer detection.

1. INTRODUCTION

Prostate cancer is the most prevalent type of cancer in men, and it is second only to lung cancer in mortality among adult males in the United States. The number of deaths in 2008 was estimated as 28,660 while the new cases diagnosed was calculated as 186,320 [1]. Early and accurate detection is important to reduce mortality and to prevent side effects from local symptoms such as bleeding, urinary tract obstruction and development of metastases. Current prostate cancer diagnosis relies on a combination of digital rectal examination (DRE), screening based on prostate specific antigen levels (PSA) and biopsy guided by transrectal ultrasound (TRUS) imaging. These methods have shown shortcomings in accuracy and specificity and, therefore, new diagnostic tools are required. DRE is limited anatomically to the posterior

c a n c d 5 (v

In this work, CrW sonoelastography is applied *ex vivo* human prostate glands to evaluate its performance in cancer detection. Image processing techniques are introduced to compensate for attenu autocorrelation methods. One of the main advantages of this method is its computational simplicity, comparable to current color flow processing available in commercial US scanners.

2.2 Enhancement of CrW images

The accuracy of the estimation of the shear velocity spatial distribution depends on the quality of the crawling waves. This section introduces a pre-processing scheme to improve the SNR of the CrW images by taking into account the time relationship among the frames of a CrW movie (cine loop) while imaging the same spatial location. An additional advantage of this processing is the generation of a quality metric which can be used to discriminate the shear velocity information accordingly. Figure 2 summarizes the proposed approach. A CrW movie is taken at a single position in the tissue. Each frame of the movie is processed using a median filter to reduce the noise. Due to the nature of CrW imaging, the median filter uses a support kernel which is larger than wider (i.e. [11x3]). Subsequently, the images are improved by 3 processes: Horizontal and vertical motion filtering, slow time filtering and a phase multiplication.

First, a horizontal motion filter [17] is applied to improve SNR and reduce potential reflection artifacts. A horizontal line from the CrW movie (blue line in Figure 3a) is followed in time to form a 2D image which would ideally look like Figure 3c. The 2D Fourier transform of such an image would have its energy concentrated in two peaks (sinusoidal in time and space) of known frequencies since the speed of the CrW and the Doppler frame rate are controlled. A band-pass filter (Figure 3d) is applied to reduce noise and artifacts. This operation is repeated for all the lines in the CrW movie. Similarly, a vertical motion filter is applied. In this case, a vertical line is followed in time to form an image, and a low-pass filter is employed since most of the energy is concentrated in the time axis.

Subsequently a slow time filter is applied to compensate for attenuation and to improve the SNR. This filter processes the signal obtained from a single spatial position (i.e. pixel) in time. Since the CrW are governed by Equation 8, the signal in each pixel should vary following a sinusoidal pattern of frequency Δw. The slow time signals are then fit into a sinusoidal model:

$$Y = A\cos(\Delta w X + \theta) + D \qquad (9)$$

where Y is the value of the slow time signal, and X is the independent variable which corresponds to the frame number. A, θ, and D are the parameters of the model to be estimated and correspond to the amplitude, phase and offset of the signal, respectively. Two images are obtained as a result of the slow time processing: A phase image and an r^2-value image. The latter represents the goodness of fit in the optimization process for each of the pixels in the CrW movie and it is employed as a quality index. Pixels with r^2 lower than 0.6 are not considered for further processing.

From the phase image, a filtered version of the CrW movie can be reconstructed. In this filtered version, the CrW have normalized amplitude and noise effects have been considerably reduced. In order to improve the estimation of shear velocity using the autocorrelation approach [16], the phase image is multiplied by a factor of four. As a consequence, the final processed CrW movie has four times the spatial frequency than its original version.

2.3 Pseudo-sonoelastographic images

Sonoelastography is a tissue elasticity imaging technique that estimates the amplitude response of tissues under harmonic mechanical excitation using ultrasonic Doppler techniques [15]. Due to the relationship between particle vibrational response and received Doppler spectral variance [18], the amplitude of low frequency shear waves propagating in tissue can be visualized in real-time using sonoelastography to detect regions of abnormal stiffness [19]. Clinical research in sonoelastography has focused primarily on prostate cancer detection. An initial comparison between sonoelastographic images and corresponding histological slides with promising results was reported by Rubens et al. in 1995 [20]. An experimental setup for three-dimensional sonoelastography was built by Taylor and colleagues. Their results indicated that sonoelastography had the capability to detect lesions over 1cc [5]. More recently initial results of undergoing studies have been presented, including an extension to in vivo imaging [12]. It is possible to reconstruct an image equivalent to the sonoelastographic image from a CrW movie. This pseudo-sonoelastographic image is created by taking the maximum of the same signal used in slow time filtering: The maximum of the values each pixel takes over time. Therefore it is possible to compare results from CrW and (pseudo) sonoelastographic images.

3. MATERIALS AND METHODS

3.1 Simulations

A CrW movie on a homogeneous media was simulated to test the performance of the motion filtering, slow time filtering and phase multiplication stages under the presence of noise and reflection artifacts. The estimation of the shear velocity using the local autocorrelation method was compared with no filtering, only slow-time filtering, and both motion and slow-time filtering. In addition, the changes in the estimation were compared with and without phase multiplication.

3.2 Experiments

Table 1 summarizes the performances of CrW sonoelastography and pseudo-sonoelastography for prostate cancer detection in terms of accuracy, sensitivity and specificity. Three cross-sections from each of the fifteen prostate glands were analyzed. Out the forty-five samples, four were discarded due to poor SNR. These cross-sections were closed to the base of the gland (AB3) and showed a very low quality metric (<0.6). CrW sonoelastography outperforms pseudo-sonoelastography. The shear velocity for all included cancerous and normal tissues was estimated as 4.75±0.97 m/s and 3.26±0.87 m/s, respectively.

In order to understand the viscoelastic effect in the range of frequencies used (100-140Hz), five cross-sections that contained no detectable cancer were analyzed. Results from this quantitative analysis are shown in Table 2. The increment in shear velocity with frequency is indicative of a viscoelastic effect.

5. DISCUSSION

ACKNOWLEDGEMENTS

The authors would like to thank GE Ultrasound for their support and Dr. Jay Hah for his comments on the final manuscript. This work was funded by NIH Grant 5R01AG016317-07.

REFERENCES

[1] American Cancer Society - Cancer Facts and Figures 2008, American Cancer Society (2008).

[2] Reissigl, A., Pointner, J., Strasser, H., Ennemoser, O., Klocker H., and Bartsch, G., "Frequency and clinical significance of transition zone cancer in prostate cancer screening," Prostate, 30, 130–135 (1997).

[3] Benson, M.C. and Olsson, C.A., "Prostate specific antigen and prostate specific antigen density: Roles in patient evaluation and management," Cancer, 74, 1667-1673 (1994).

[4] Ellis, W.J. and Brawer, M.K., "The significance of isoechoic prostatic carcinoma," J. Urol., 152, 2304–2307 (1994).

[5] Taylor, L.S., Rubens, D.J., Porter, B.C., Wu, Z., Baggs, R.B., di Sant'Agnese, P.A., et al., "Prostate cancer: Sonoelastography for in vitro detection", Radiology, 237, 981-985 (2005).

[6] Gao, L., Parker, K.J., Lerner, R.M., and Levinson, S.F., "Imaging of the elastic properties of tissue - A review," Ultrasound Med. Biol., 22, 959-977 (1996).

[7] Ophir, J., Alam, S.K., Garra, B., Kallel, F., Konofagou E., Krouskop, T., and Varghese, T., "Elastography: Ultrasonic estimation and imaging of the elastic properties of tissues," Proc. Instn. Mech. Engrs., 213, 203-233 (1999).

[8] Greenleaf, J., Fatemi, M., and Insana, M., "Selected methods for imaging elastic properties of biological tissues," Annu. Rev. Biomed. Eng., 5, 57-78 (2003).

[9] Lorenz, A., Sommerfeld, H., Garcia-Schurmann, M., Philippou, S., Senge, T., and Ermert, H., "A new system for the acquisition of ultrasonic multicompression strain images of the human prostate in vivo," IEEE Trans. Ultrason. Ferroelec. Freq. Contr., 46, 1147-1153 (1999).

[10] Pesavento, A., and Lorenz, A., "Real time strain imaging and in vivo applications in prostate cancer," Proc. IEEE Ultrason. Symp., 2, 1647-1652 (2001).

[11] Souchon, R., Rouviere, O., Gelet, A., Detti, V., Srinivasan, S., Ophir, J., and Chapelon, J.Y., "Visualisation of HIFU lesions using elastography of the human prostate in vivo: Preliminary results," Ultrasound Med. Biol., 29, 1007-1015 (2003).

[12] Hoyt, K., Castaneda. B., Zhang. M., Nigwekar. P., di Sant'Agnese. P.A., Joseph. J.V., Strang. J., Rubens. D.J., Parker. K.J., "Tissue elasticity properties as biomarkers for cancer in prostate," Cancer Biomarkers, 4, 213-225 (2008).

[13]

[21] Castaneda, B., Tamez-Pena, J.G., Zhang, M., Hoyt, K., Bylund, K., Christensen, J., Saad, W., Strang, J., Rubens, D.J., and Parker, K.J., "Measurement of thermally-ablated lesions in sonoelastographic images using level set methods," Proceedings of SPIE, 6920, 692018-1 - 692018-8 (2008).

[22] Zhang, M., Nigwekar, P., Castaneda, B., Hoyt, K., Joseph, J.V., di Sant'agnese, A., Messing, E.M., Strang, J.G., Rubens, D.J., and Parker, K.J., "Quantitative characterization of viscoelastic properties of human prostate correlated with histology," Journal of Ultrasound in Medicine, 34, 1033-1042 (2008).

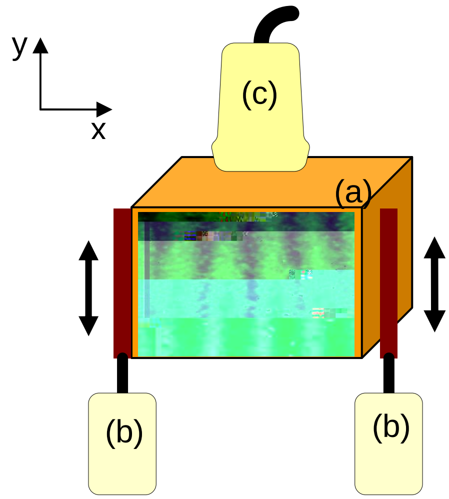

Figure 1. Schematic of the experimental setup. The prostate gland embedded in a gelatin mold (a) is located between two shear vibration sources (b). The ultrasound transducer is positioned on top to acquire the crawling wave images (c).

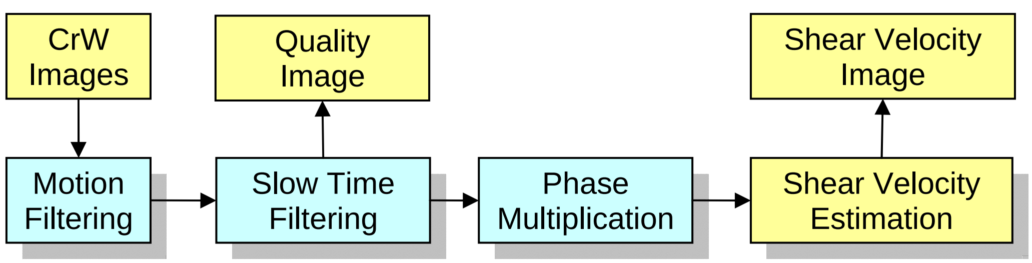

Figure 2. Proposed scheme to enhance the crawling wave images.

(a) (b)

(c) (d)

(a) (b) (c)

Figure 4. Results from the shear velocity es